N71-17253

NASA TM X-2205

NASA TECHNICAL MEMORANDUM

NASA TM X-2205

LONGITUDINAL AERODYNAMIC CHARACTERISTICS OF THE VIKING LANDER CAPSULE AT MACH 6

by Theodore J. Goldberg and James C. Emery

Langley Research Center
Hampton, Va. 23365

NATIONAL AERONAUTICS AND SPACE ADMINISTRATION • WASHINGTON, D. C. • FEBRUARY 1971

1. Report No. NASA TM X-2205	2. Government Accession No.	3. Recipient's Catalog No.
4. Title and Subtitle LONGITUDINAL AERODYNAMIC CHARACTERISTICS OF THE VIKING LANDER CAPSULE AT MACH 6		5. Report Date February 1971
		6. Performing Organization Code
7. Author(s) Theodore J. Goldberg and James C. Emery		8. Performing Organization Report No. L-7516
		10. Work Unit No. 815-20-09-08
9. Performing Organization Name and Address NASA Langley Research Center Hampton, Va. 23365		11. Contract or Grant No.
		13. Type of Report and Period Covered Technical Memorandum
12. Sponsoring Agency Name and Address National Aeronautics and Space Administration Washington, D.C. 20546		14. Sponsoring Agency Code
15. Supplementary Notes		

16. Abstract

An investigation of the longitudinal aerodynamic characteristics of a 0.0348-scale Viking lander capsule has been conducted at a Mach number of 6 and free-stream Reynolds numbers from 0.98×10^7 to 2.35×10^7 per meter. Data obtained at angles of attack from -3° to 20° were compared with analytical values obtained by the $\sin^2$ deficiency method and modified Newtonian theory.

17. Key Words (Suggested by Author(s))		18. Distribution Statement	
Viking Space vehicle		Unclassified – Unlimited	
19. Security Classif. (of this report) Unclassified	20. Security Classif. (of this page) Unclassified	21. No. of Pages 17	22. Price* $3.00

*For sale by the National Technical Information Service, Springfield, Virginia 22151

LONGITUDINAL AERODYNAMIC CHARACTERISTICS OF THE VIKING LANDER CAPSULE AT MACH 6

By Theodore J. Goldberg and James C. Emery
Langley Research Center

SUMMARY

An investigation of the longitudinal aerodynamic characteristics of a 0.0348-scale Viking lander capsule has been conducted at a Mach number of 6 and free-stream Reynolds numbers from 0.98×10^7 to 2.35×10^7 per meter.

The results indicated that the Reynolds number had no effect on the aerodynamic coefficients. The afterbody had no effect on the aerodynamic coefficients for angles of attack from -3° to 20°. The $\sin^2$ deficiency method predicts the longitudinal aerodynamic coefficients resonably well, whereas the modified Newtonian theory overpredicts the normal-force and pitching-moment coefficients.

INTRODUCTION

The Viking missions are part of a group of missions directed toward the exploration of the planet Mars by means of automated spacecraft. Uncertainties about the Mars atmosphere necessitate that design considerations for the Viking lander capsule (VLC) encompass a large range of aerodynamic conditions. Experimental investigations of the VLC aerodynamic characteristics are required because of the paucity of experimental data and the uncertainty of utilizing analytical methods for predicting the hypersonic longitudinal aerodynamic characteristics of the configuration. The experimental determination of these coefficients throughout the Mach number range is necessary to provide the input data for trajectory analysis and for design of the mission and subsystems. Experimental results for the VLC at Mach numbers of 14 and 20 are presented in reference 1.

This paper presents the results of tests conducted in the Langley 20-inch Mach 6 tunnel to obtain longitudinal force and moment data on the Viking lander capsule. This investigation was conducted at free-stream Reynolds numbers from 0.98×10^7 to 2.35×10^7 per meter over an angle-of-attack range from -3° to 20°.

SYMBOLS

Forces and moments are referred to the body-axis system except for lift and drag, which are referred to the wind-axis system. (See fig. 1.) Moments are taken about the center of gravity.

C_A	axial-force coefficient, $F_A/q_\infty S$
C_D	drag coefficient, $C_A \cos\alpha + C_N \sin\alpha$
C_L	lift coefficient, $C_N \cos\alpha - C_A \sin\alpha$
C_m	pitching-moment coefficient, $M_Y/q_\infty Sd$
C_N	normal-force coefficient, $F_N/q_\infty S$
$C_{p,b}$	base-pressure coefficient, $\dfrac{p_b - p_\infty}{q_\infty}$
d	model reference diameter, 12.192 cm
F_A	force along X-axis
F_N	force along Z-axis
L/D	lift-drag ratio, C_L/C_D
M	Mach number
M_Y	moment about Y-axis
p	pressure
q	dynamic pressure
R	Reynolds number
S	reference area, $\pi d^2/4$, 116.748 cm^2
T	temperature

X, Y, Z body-axis system (fig. 1)

x_{cg} distance from theoretical apex of the 140° cone to center of gravity (moment reference), measured along the X-axis, 0.23d

x_{cp} distance from theoretical apex of the 140° cone to center of pressure, $x_{cg} - \frac{C_m}{C_N} d$

α angle of attack

Subscripts:

av average

b base

t total or stagnation

∞ free stream

APPARATUS AND METHODS

Model

Drawings and details of the 0.0348-scale model of the Viking lander capsule are shown in figure 2. The forebody is a cone with 140° included angle and a spherical nose. It is mounted base to base with an afterbody composed of two truncated cones having included angles of 80° and 124.36°, respectively. The juncture of the forebody and afterbody is at the maximum model diameter (2.278 cm from the theoretical apex of the forebody). The model was constructed of stainless steel but hollowed for weight reduction. The model consisting of the forebody and base plate is called the aeroshell. The model consisting of the forebody and afterbody is referred to as the Viking lander capsule (VLC). Photographs of the VLC and the component parts of the aeroshell and the VLC are presented in figure 3.

Wind Tunnel

This investigation was conducted in the Langley 20-inch Mach 6 tunnel. This blowdown tunnel, which is described in reference 2, is capable of operating at stagnation pressures from 0.34 to 3.62 MN/m^2 and a maximum stagnation temperature of 560° K. The

Mach number is achieved with fixed two-dimensional nozzle blocks forming a test section 52.07 cm high and 50.80 cm wide with a test core of approximately 38 cm by 38 cm. The air is heated by an electrical resistance heater to avoid liquefaction. The tunnel is equipped with a movable second minimum and exhausts either into the atmosphere with the aid of an annular air ejector or into a vacuum sphere.

Tests

The tests were conducted at a nominal free-stream Mach number of 6 at stagnation pressures from 1.21 to 2.76 MN/m^2 and a stagnation temperature of 478° K. The corresponding free-stream Reynolds numbers were from 0.98×10^7 to 2.35×10^7 per meter. Data were obtained over an angle-of-attack range from -3° to 20°. The test conditions for the runs used in the present paper are given in table I. The model was tested with and without the afterbody.

Methods and Instrumentation

The aerodynamic forces and moments were measured by means of a water-cooled six-component electrical strain-gage balance housed inside the model. The balance was rigidly connected to the sting support system, which was pneumatically driven through an angle-of-attack range in the vertical plane during the run. The portion of the balance extending rearward of the aeroshell configuration was covered with a shield to prevent flow impingement on the balance.

The true angles of attack were set optically by means of a point source of light and a small lens-prism mounted on the rear of the model. The image of the light source was reflected by the prism and focused by the lens onto a calibrated screen.

Six base-pressure orifices 0.119 cm in diameter were located in the afterbody as shown in figure 2. Model base pressures were measured during separate runs at Reynolds numbers of 0.98×10^7 and 2.35×10^7 per meter.

The Mach number was obtained from a pitot-pressure probe which could be injected into and retracted from the flow. During the base-pressure tests this probe was left in the flow and a Mach number was, therefore, obtained for each angle of attack. During the force tests the probe was in the flow only at the beginning and end of each run to avoid possible interference; therefore, a linear variation of Mach number was used to compute the force coefficients for each angle of attack.

The base pressures and the pitot probe were connected to individual multirange capacitance-type pressure transducers. Each pressure was monitored by an automatic range selector which chose the range closest to the measured value. Tunnel stagnation pressures were measured with strain-gage transducers that had ranges of 0 to 1.38, 0 to 2.1, and 0 to 3.4 MN/m^2. All pressure, temperature, and force and moment data of this investigation were recorded on magnetic tape for processing by an electronic system; however, the data were also visually monitored during each run.

Accuracy

On the basis of accuracy in balance calibration, computer readout, dynamic pressure, and pressure transducers, the uncertainties in the force and moment coefficients, as estimated by a method of least squares, are as follows:

C_N	±0.005	C_L	±0.007
C_A	±0.028	C_D	±0.028
C_m	±0.001	L/D	±0.008

The accuracy of the base-pressure coefficients is estimated to be ±0.001. The accuracy of the angles of attack is estimated to be $\pm 0.1^{\circ}$ and the free-stream Mach number is estimated to be accurate to ±0.02.

RESULTS AND DISCUSSION

The results of these tests are presented as coefficients of forces, moments, and base pressures in tables and comparison plots. The measured base-pressure coefficients are given in table II. The measured aerodynamic force and moment coefficients are given in table III.

Figure 4 presents the variation of the base-pressure coefficients with angle of attack for each orifice as well as the arithmetic average for the six orifices. Reynolds number has very little effect on the base-pressure coefficient. As has been shown in reference 3, at Mach numbers greater than about 3 the base pressure generally decreases with increasing Reynolds number until the boundary layer becomes fully turbulent and then remains approximately constant for further increases in Reynolds number. The average base-pressure coefficients are approximately 65 percent of $-1/M_{\infty}^2$. The variations of the basic longitudinal aerodynamic characteristics with angle of attack and Reynolds number for the Viking lander capsule and the aeroshell are presented in figures 5 and 6. In these figures the axial-force coefficients have been adjusted to correspond to a base pressure equal to free-stream static pressure. It can be seen from figure 5 that Reynolds number has no effect on the aerodynamic coefficients (data scatter is within the accuracy of these tests). A comparison of figures 5 and 6 indicates that the afterbody has no effect on the aerodynamic coefficients over the angle-of-attack range investigated.

The longitudinal aerodynamic coefficients of the present investigation were computed from pressure distributions obtained by the $\sin^2$ deficiency method of references 4 and 5 and by using the modified Newtonian theory in the hypersonic arbitrary-body aerodynamic computer program of references 6 and 7. For calculations by the $\sin^2$ deficiency method, the stagnation points were assumed to be at the same locations as those used in reference 5 and can be obtained from reference 8. The integral equations of reference 9 were used to obtain the force and moment coefficients from the pressure distributions. Comparison of the measured and calculated values in figures 5 and 6 shows that the $\sin^2$ deficiency method predicts the longitudinal characteristics of this type of body reasonably well up to an angle of attack of nearly 20°, whereas the modified Newtonian theory overpredicts the normal-force and pitching-moment coefficients.

Typical schlieren photographs of the Viking lander capsule are presented in figure 7 to show the change in shock shape with angle of attack.

CONCLUDING REMARKS

An investigation has been conducted to determine the longitudinal aerodynamic characteristics of a 0.0348-scale Viking lander capsule at a Mach number of 6 and free-stream Reynolds numbers from 0.98×10^7 to 2.35×10^7 per meter. Neither the Reynolds number nor the afterbody affects the longitudinal aerodynamic coefficients at angles of attack from -3° to 20°. The $\sin^2$ deficiency method predicts the longitudinal aerodynamic coefficients reasonably well for angles of attack up to nearly 20°, whereas the modified Newtonian theory overpredicts the normal-force and pitching-moment coefficients.

Langley Research Center,
National Aeronautics and Space Administration,
Hampton, Va., January 15, 1971.

REFERENCES

1. Blake, W. W.: Hypersonic Experimental Static Aerodynamic Characteristics of Viking Lander Capsule. TR-3709012 (Contract NAS1-9000), Martin Marietta Corp., May 8, 1970.

2. Sterrett, James R.; and Emery, James C.: Extension of Boundary-Layer-Separation Criteria to a Mach Number of 6.5 by Utilizing Flat Plates With Forward-Facing Steps. NASA TN D-618, 1960.

3. Staylor, W. Frank; and Goldberg, Theodore J.: Afterbody Pressures on Boattailed Bodies of Revolution Having Turbulent Boundary Layers at Mach 6. NASA TN D-2761, 1965.

4. Love, E. S.; Woods, W. C.; Rainey, R. W.; and Ashby, G. C., Jr.: Some Topics in Hypersonic Body Shaping. AIAA Pap. 69-181, Jan. 1969.

5. Stallings, Robert L., Jr.; and Campbell, James F.: An Approximate Method for Predicting Pressure Distributions on Blunt Bodies at Angle of Attack. J. Spacecraft Rockets, vol. 7, no. 11, Nov. 1970, pp. 1306-1310.

6. Gentry, Arvel E.: Hypersonic Arbitrary-Body Aerodynamic Computer Program. Vol. 1 – User's Manual. Rep. DAC 56080 (Air Force Contract No. F33615 67 C 1008), Douglas Aircraft Co., Mar. 1967. (Available from DDC as AD817158.)

7. Gentry, Arvel E.: Hypersonic Arbitrary-Body Aerodynamic Computer Program. Vol. II – Program Formulation and Listings. Rep. DAC 56080 (Air Force Contract No. F33615 67 C 1008), Douglas Aircraft Co., Mar. 1967. (Available from DDC as AD817159.)

8. Campbell, James F.; and Tudor, Dorothy H.: Pressure Distributions on 140°, 160°, and 180° Cones at Mach Numbers From 2.30 to 4.63 and Angles of Attack From 0° to 20°. NASA TN D-5204, 1969.

9. Stallings, Robert L., Jr.; and Tudor, Dorothy H.: Experimental Pressure Distributions on a 120° Cone at Mach Numbers From 2.96 to 4.63 and Angles of Attack From 0° to 20°. NASA TN D-5054, 1969.

TABLE I.- TEST CONDITIONS

[α = -3^o to 20^o]

Run	$p_{t,\infty}$, MN/m^2	$T_{t,\infty}$, ^oK	R_∞ per meter	M_∞	Model
Base pressure					
1	2.79	478	2.35×10^7	6.02	VLC
2	1.17	480	.98	6.02	VLC
Aerodynamic characteristics					
11	2.79	478	2.35×10^7	5.99	Aeroshell
12	1.17	472	1.00	5.99	Aeroshell
16	2.79	479	2.35	5.99	VLC
17	2.00	478	1.67	5.99	VLC
18	1.17	479	.98	5.99	VLC

TABLE II.- BASE PRESSURES

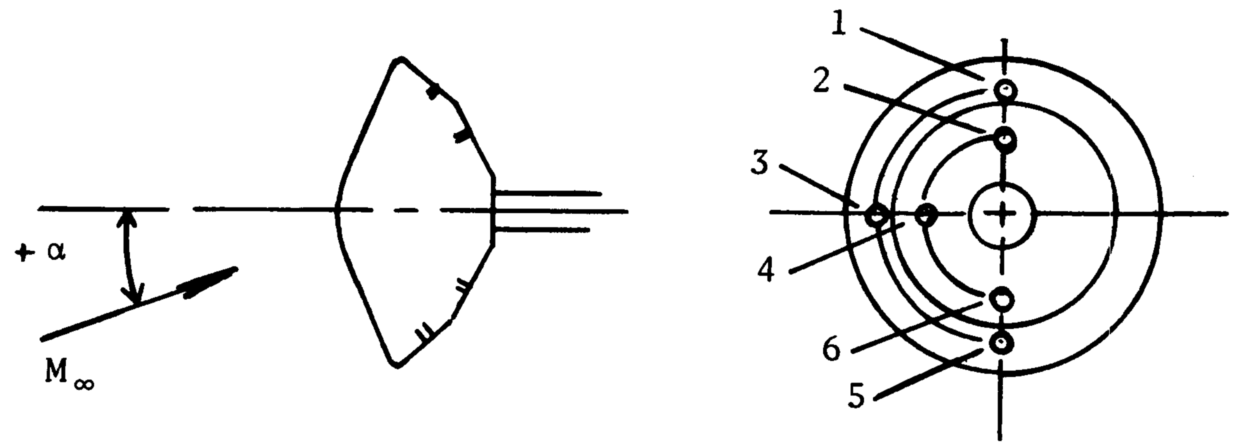

Run	α, deg	$p_{b,1}$, kN/m^2	$(C_{p,b})_1$	$p_{b,2}$, kN/m^2	$(C_{p,b})_2$	$p_{b,3}$, kN/m^2	$(C_{p,b})_3$	$p_{b,4}$, kN/m^2	$(C_{p,b})_4$	$p_{b,5}$, kN/m^2	$(C_{p,b})_5$	$p_{b,6}$, kN/m^2	$(C_{p,b})_6$	$p_{b,av}$, kN/m^2	$(C_{p,b})_{av}$
1	-2.84	1.01	-0.017	0.91	-0.019	1.03	-0.016	0.93	-0.018	1.24	-0.012	1.33	-0.009	1.072	-0.015
	-.84	.92	-.018	.86	-.019	.95	-.017	.90	-.019	.98	-.017	.99	-.016	.934	-.018
	.16	1.04	-.015	.97	-.017	.97	-.017	.91	-.018	.92	-.018	.92	-.018	.956	-.017
	1.16	1.17	-.013	1.17	-.012	.95	-.017	.88	-.019	.93	-.018	.90	-.019	1.000	-.016
	3.16	1.20	-.012	1.17	-.012	.96	-.017	.90	-.019	.96	-.017	.91	-.018	1.017	-.016
	6.16	1.07	-.014	.96	-.017	.94	-.018	.89	-.019	.93	-.018	.91	-.018	.961	-.017
	9.16	.95	-.017	.86	-.019	.86	-.019	.83	-.020	.86	-.019	.86	-.019	.870	-.019
	12.16	.95	-.017	.90	-.018	.87	-.019	.85	-.019	.85	-.019	.84	-.020	.889	-.019
	15.16	.94	-.017	.79	-.021	.86	-.019	.79	-.021	.80	-.020	.83	-.020	.834	-.020
	20.16	.91	-.018	.76	-.021	.83	-.020	.76	-.021	.77	-.021	.81	-.020	.807	-.020
2	-2.84	0.44	-0.015	0.44	-0.016	0.44	-0.015	0.47	-0.015	0.47	-0.013	0.47	-0.013	0.444	-0.015
	-.84	.45	-.015	.44	-.016	.44	-.015	.43	-.015	.43	-.015	.43	-.015	.437	-.015
	.16	.46	-.014	.44	-.015	.44	-.016	.42	-.016	.42	-.016	.43	-.016	.439	-.015
	1.16	.49	-.013	.43	-.013	.43	-.015	.43	-.015	.43	-.015	.43	-.016	.449	-.014
	3.16	.48	-.013	.43	-.013	.43	-.016	.43	-.016	.43	-.016	.43	-.016	.445	-.015
	6.16	.44	-.015	.40	-.016	.42	-.017	.41	-.016	.41	-.016	.42	-.016	.417	-.016
	9.16	.43	-.015	.40	-.017	.41	-.017	.41	-.017	.41	-.017	.42	-.016	.411	-.017
	12.16	.44	-.015	.41	-.017	.41	-.017	.41	-.017	.41	-.017	.42	-.016	.416	-.017
	15.16	.45	-.014	.42	-.017	.41	-.016	.40	-.017	.40	-.017	.424	-.016	.415	-.016
	20.16	.44	-.016	.40	-.018	.40	-.018	.37	-.018	.37	-.019	.414	-.017	.399	-.018

TABLE III.- AERODYNAMIC CHARACTERISTICS

(a) Viking lander capsule

Run	α, deg	C_N	C_A	C_m	C_L	C_D	L/D	x_{cp}/d
16	-2.84	-0.0040	1.6146	0.0047	0.0760	1.6129	0.047	
	-.84	-.0001	1.6163	.0006	.0236	1.6161	.015	
	.16	.0021	1.6154	-.0016	-.0024	1.6154	-.001	[a] 1.234
	2.16	.0056	1.6155	-.0051	-.0553	1.6146	-.034	
	4.16	.0104	1.6087	-.0090	-.1063	1.6052	-.066	1.091
	6.16	.0160	1.6010	-.0129	-.1559	1.5935	-.098	1.036
	8.16	.0214	1.5927	-.0165	-.2049	1.5796	-.130	1.000
	10.16	.0262	1.5812	-.0200	-.2531	1.5610	-.162	.994
	12.16	.0311	1.5657	-.0239	-.2994	1.5372	-.195	.998
	14.16	.0368	1.5450	-.0278	-.3423	1.5071	-.227	.986
	17.16	.0435	1.5054	-.0337	-.4026	1.4512	-.277	1.005
	20.16	.0541	1.4520	-.0410	-.4496	1.3817	-.325	.988
17	-2.84	-0.0052	1.5959	0.0053	0.0739	1.5942	0.046	
	.84	-.0012	1.5993	.0014	.0222	1.5992	.014	
	.16	.0008	1.6000	-.0007	-.0037	1.6000	-.002	[a] 1.285
	2.16	.0041	1.5984	-.0046	-.0562	1.5974	-.035	
	4.16	.0089	1.5929	-.0083	-.1067	1.5893	-.067	1.161
	6.16	.0148	1.5871	-.0122	-.1556	1.5795	-.098	1.054
	8.16	.0204	1.5774	-.0160	-.2037	1.5643	-.130	1.015
	10.16	.0250	1.5674	-.0196	-.2518	1.5472	-.163	1.013
	12.16	.0299	1.5511	-.0233	-.2975	1.5226	-.195	1.010
	14.16	.0348	1.5336	-.0271	-.3414	1.4956	-.228	1.010
	17.16	.0422	1.4920	-.0334	-.3999	1.4380	-.278	1.023
	20.16	.0518	1.4394	-.0406	-.4475	1.3691	-.327	1.014
18	-2.84	-0.0093	1.5940	0.0065	0.0697	1.5925	0.044	
	-.84	-.0044	1.5981	.0022	.0190	1.5980	.012	
	.16	-.0024	1.5990	.0004	-.0069	1.5990	-.004	[a] 1.169
	2.16	.0003	1.5993	-.0032	-.0600	1.5982	-.038	
	4.16	.0059	1.5926	-.0071	-.1096	1.5888	-.069	
	6.16	.0109	1.5859	-.0110	-.1593	1.5779	-.101	1.239
	8.16	.0170	1.5789	-.0148	-.2073	1.5653	-.132	1.102
	10.16	.0211	1.5677	-.0185	-.2557	1.5468	-.165	1.108
	12.16	.0262	1.5524	-.0224	-.3014	1.5231	-.198	1.085
	14.16	.0328	1.5316	-.0271	-.3428	1.4931	-.230	1.054
	17.16	.0383	1.4949	-.0326	-.4044	1.4397	-.281	1.080
	20.16	.0490	1.4408	-.0404	-.4506	1.3694	-.329	1.054

(b) Aeroshell

Run	α, deg	C_N	C_A	C_m	C_L	C_D	L/D	x_{cp}/d
11	-2.84	-0.0048	1.5911	0.0049	0.0740	1.5894	0.047	
	-.84	.0001	1.5928	.0007	.0234	1.5926	.015	
	.16	.0022	1.5928	-.0011	-.0023	1.5928	-.001	[a] 1.063
	2.16	.0069	1.5905	-.0050	-.0530	1.5896	-.033	
	4.16	.0117	1.5874	-.0090	-.1035	1.5840	-.065	.998
	6.16	.0171	1.5821	-.0127	-.1528	1.5748	-.097	.974
	8.16	.0218	1.5715	-.0163	-.2015	1.5587	-.129	.978
	10.16	.0265	1.5572	-.0199	-.2486	1.5374	-.162	.980
	12.16	.0320	1.5380	-.0237	-.2927	1.5103	-.194	.971
	14.16	.0368	1.5182	-.0274	-.3357	1.4810	-.227	.975
	17.16	.0452	1.4782	-.0341	-.3929	1.4258	-.276	.984
	20.16	.0553	1.4351	-.0408	-.4427	1.3663	-.324	.968
12	-2.84	-0.0056	1.5805	0.0053	0.0727	1.5788	0.046	
	-.84	-.0008	1.5863	.0014	.0224	1.5861	.014	
	.16	.0013	1.5847	-.0005	-.0031	1.5846	-.002	[a] 1.063
	2.16	.0059	1.5847	-.0043	-.0538	1.5838	-.034	
	4.16	.0105	1.5841	-.0081	-.1044	1.5807	-.066	1.004
	6.16	.0160	1.5767	-.0121	-.1533	1.5693	-.098	.988
	8.16	.0209	1.5674	-.0157	-.2018	1.5545	-.130	.982
	10.16	.0250	1.5537	-.0192	-.2495	1.5337	-.163	.999
	12.16	.0311	1.5340	-.0232	-.2927	1.5061	-.194	.976
	14.16	.0351	1.5157	-.0270	-.3368	1.4782	-.228	1.000
	17.16	.0445	1.4749	-.0338	-.3927	1.4223	-.276	.990
	20.16	.0545	1.4315	-.0409	-.4422	1.3626	-.325	.981

[a] Obtained from slope of C_m versus C_N at $\alpha = 0^{\circ}$.

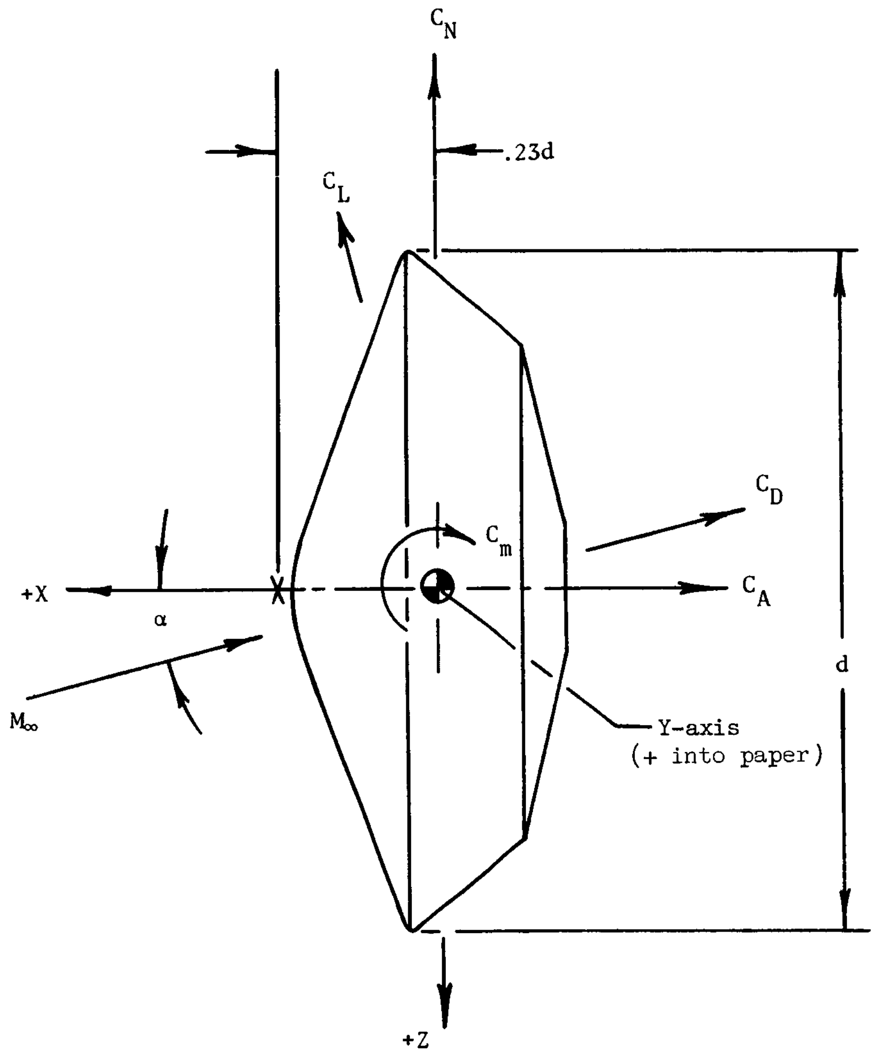

Figure 1.- Aerodynamic axes and symbols.

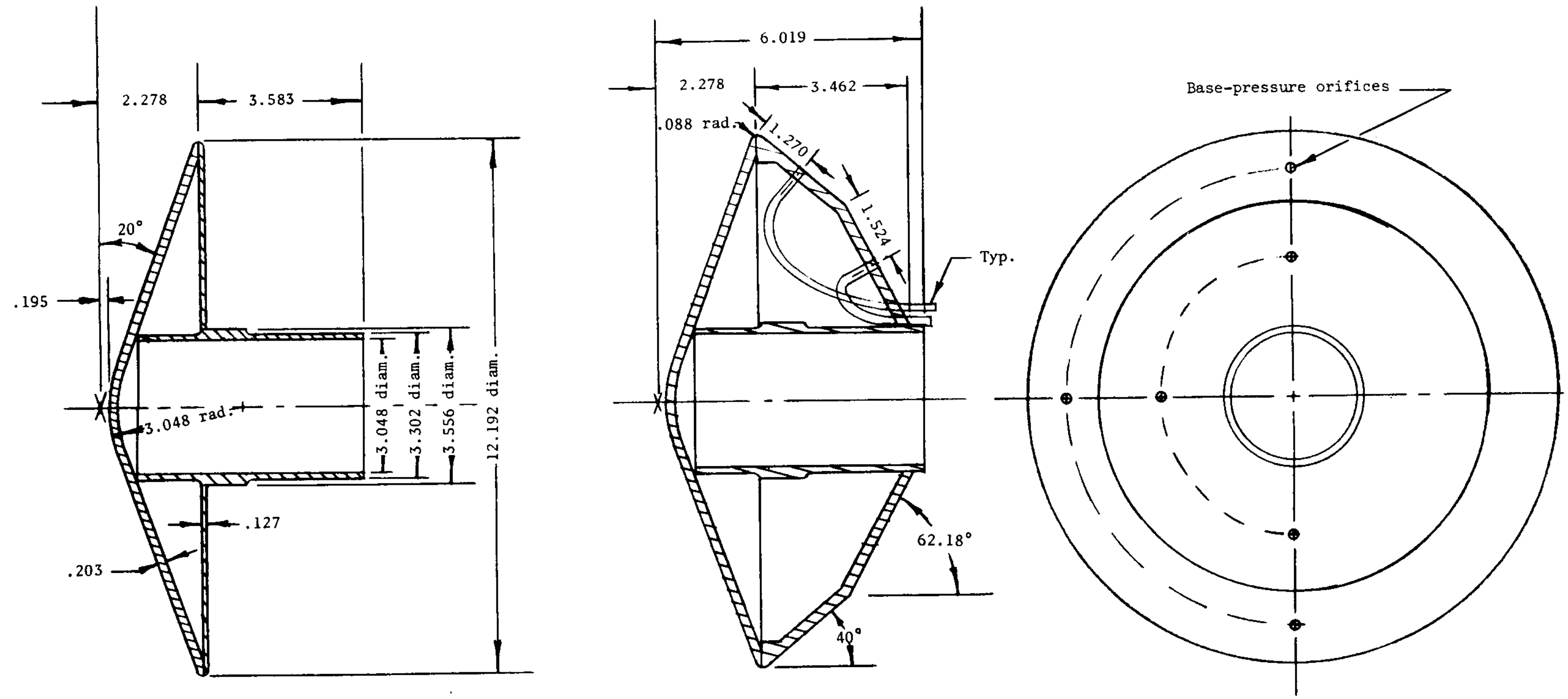

(a) Aeroshell.

(b) Lander capsule.

Figure 2.- Drawings and details of 0.0348-scale Viking model. All dimensions are in centimeters.

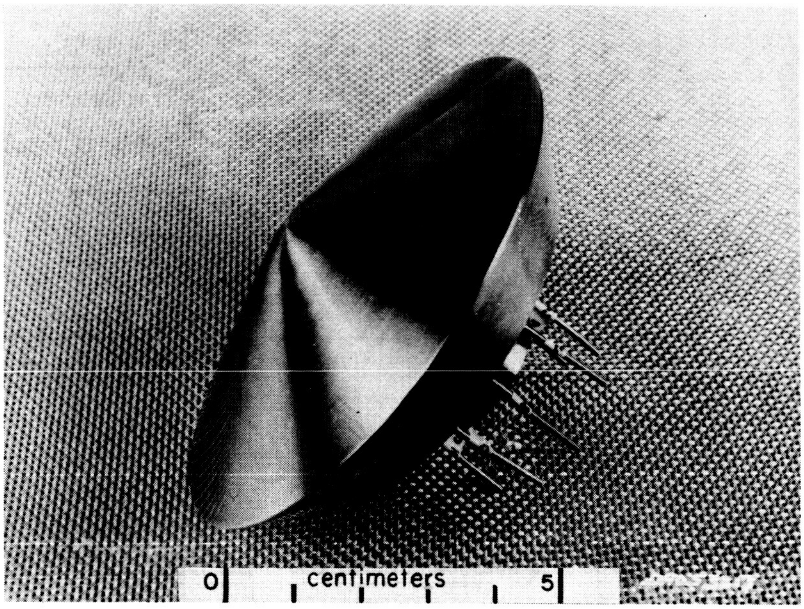

(a) VLC.

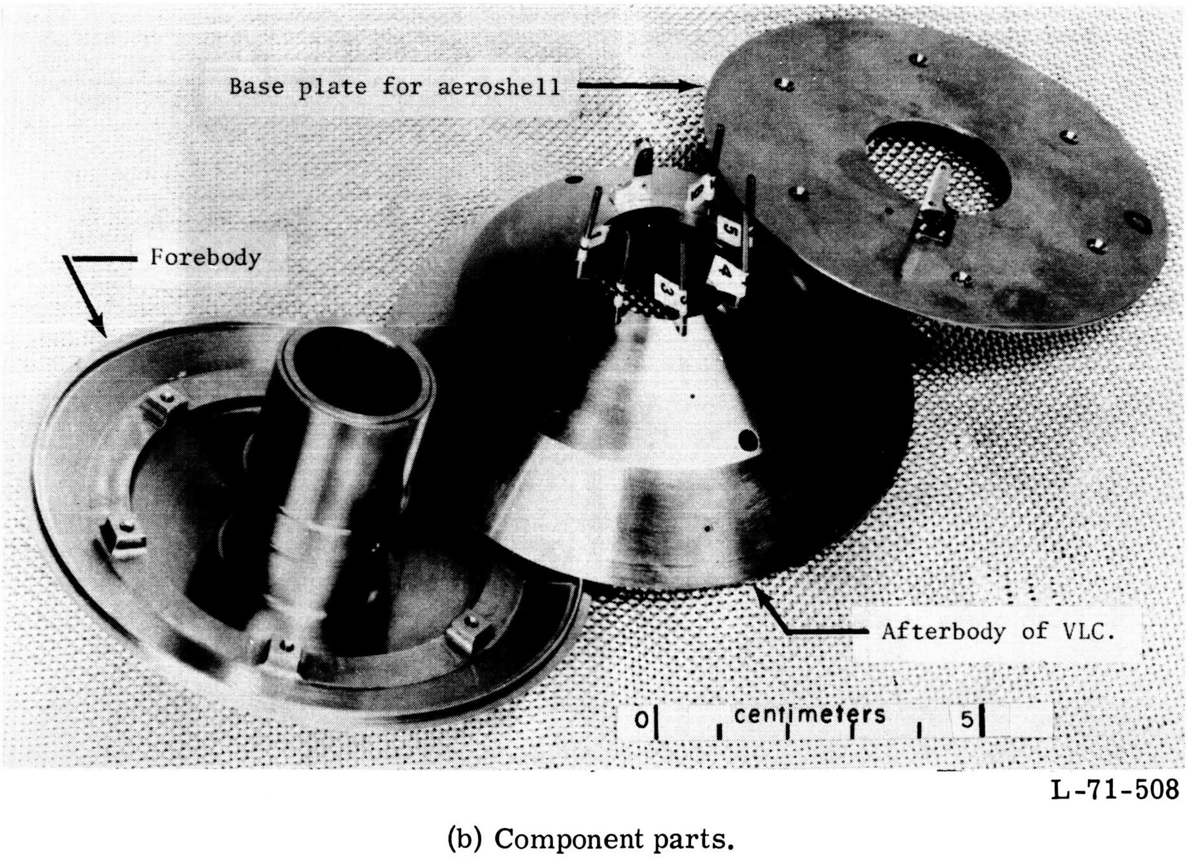

L-71-508

(b) Component parts.

Figure 3.- Photograph of Viking lander capsule and component parts.

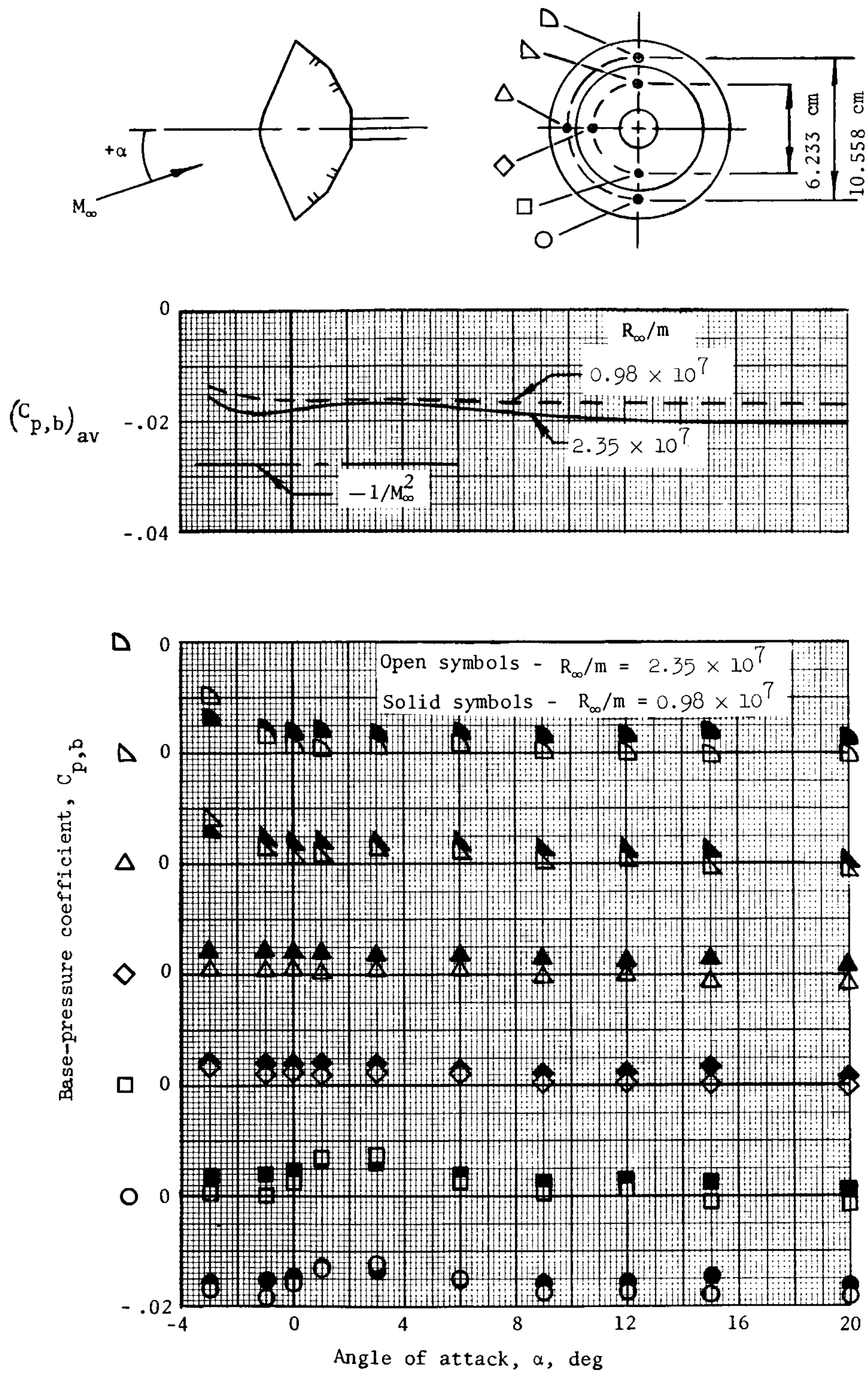

Figure 4.- Variation of base-pressure coefficient with angle of attack and Reynolds number.

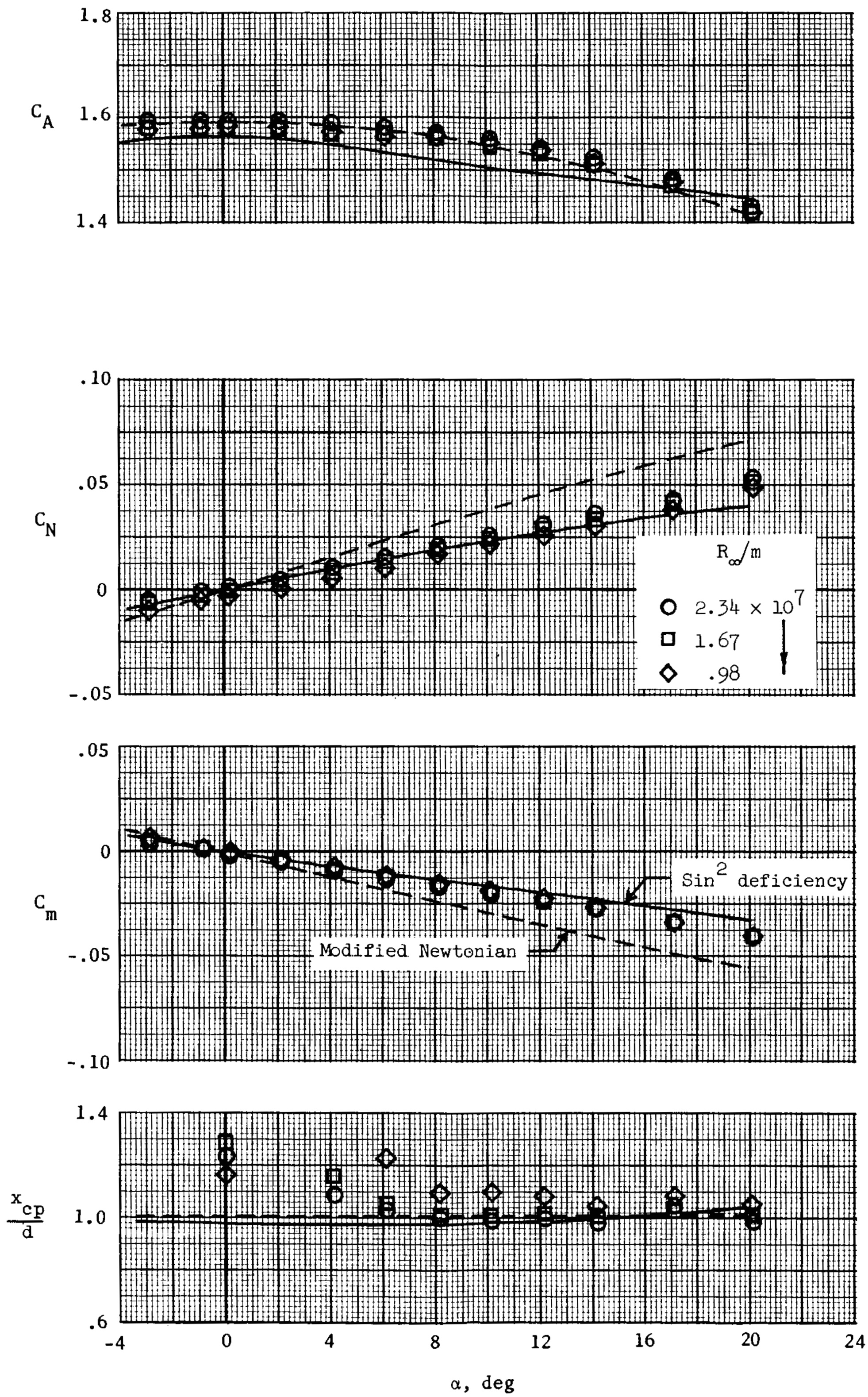

Figure 5.- Aerodynamic characteristics of the Viking lander capsule.

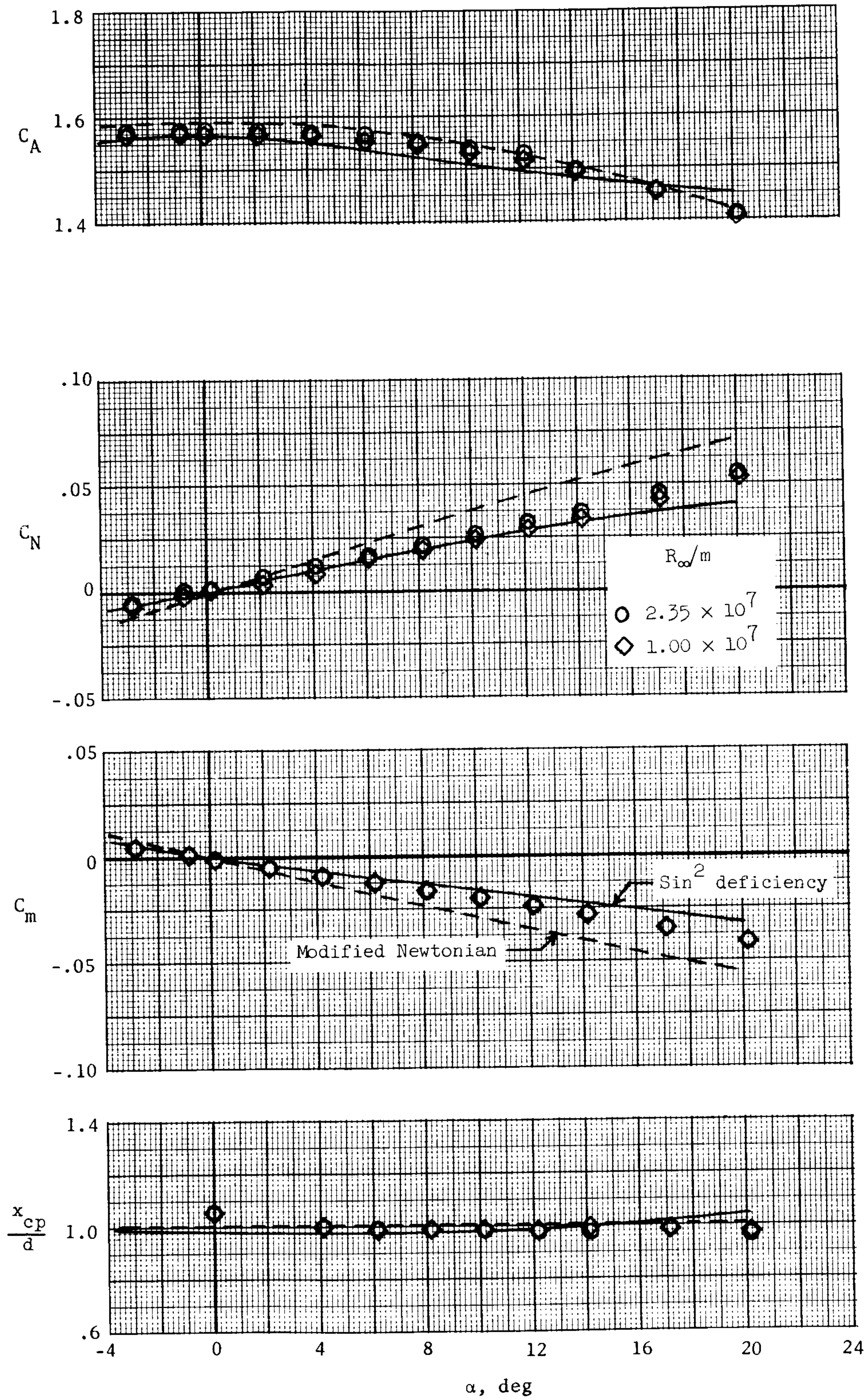

Figure 6.- Aerodynamic characteristics of the aeroshell.

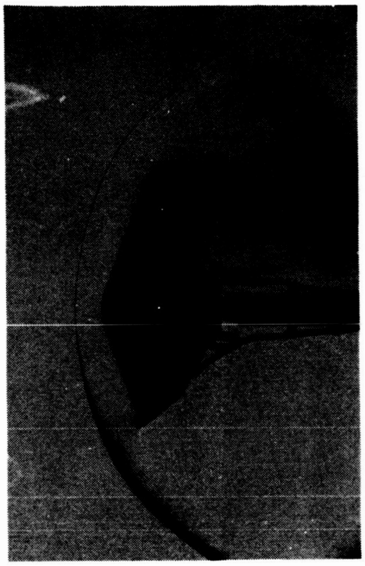

(a) $\alpha = 0^{\circ}$.

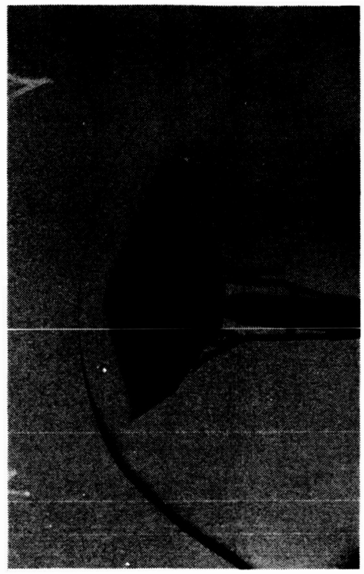

(b) $\alpha = 4^{\circ}$.

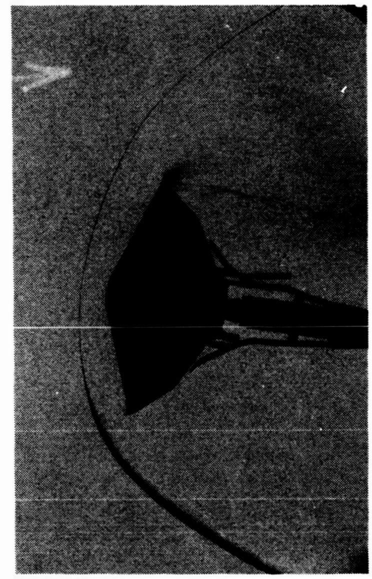

(c) $\alpha = 8^{\circ}$.

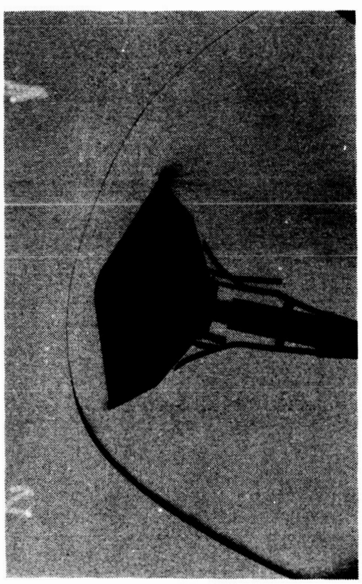

(d) $\alpha = 12^{\circ}$.

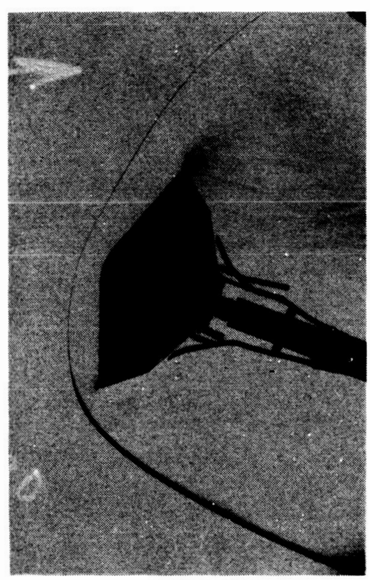

L-71-509

(e) $\alpha = 20^{\circ}$.

Figure 7.- Schlieren photographs of Viking lander capsule. $R_{\infty} = 1.67 \times 10^{7}$ per meter.